Lattice dynamics and structural instabilities of solid biphenyl and p-terphenyl-effect of pressure

1992 J. Phys.: Condens. Matter 4 6241

(http://iopscience.iop.org/0953-8984/4/29/008)

J. Phys.: Condens. Matter 4 (1992) 6241–6252. Printed in the UK

Lattice dynamics and structural instabilities of solid biphenyl and p-terphenyl—effect of pressure

T Wasiutyński† and H Cailleau

Groupe de Physique Cristalline URA au CNRS no D0804, Université de Rennes I, 35042 Rennes Cédex, France

Received 19 November 1991, in final form 2 March 1992

Abstract. The model calculations of lattice dynamics in solid biphenyl and terphenyl for different temperatures and pressures are presented. We develop a model that explicitly treats interphenyl motion in the self-consistent phonon approximation. The phase transition is interpreted as an instability (zero frequency at finite wave vector) of the twist mode with weak coupling to the external modes of the molecule. The calculations show fairly good agreement with experimental data.

1. Introduction

Since the discovery of the phase transitions in crystalline parapolyphenyls (biphenyl, p-terphenyl, ...), connected with the instability of the intramolecular modes [1], these compounds have been the subject of extensive studies, both theoretical and experimental; this is especially true of the incommensurate phases of biphenyl [2]. It is now well understood that these phase transitions are the result of competition between the intramolecular forces that tend to twist phenyl rings and the intermolecular forces that stabilize the planar conformation. The result of this competition is the instability of the mean planar molecular conformation in the high-temperature phase. It is obvious that the intramolecular mode associated with interphenyl motion has a low frequency and is strongly temperature dependent. The usual rigid molecule approximation [3] does not apply here. Since the molecular conformation changes at the phase transition, different approximations that take soft molecules into account [4, 5] are also inapplicable here. The first calculations for phonons at $q = 0$ for a solid biphenyl in the rigid phenyl ring approximation were performed by Burgos *et al* [6]; these calculations showed the importance of the mixing of internal and external biphenyl modes. However, the phase transition in biphenyl takes place far away from $q = 0$, and full lattice dynamics calculations are necessary. Subsequent models [7, 8] presented lattice dynamics calculations in the whole Brillouin zone using the non-rigid molecule approximation. The general conclusion was that the phonon branch along the b^* direction has a deep minimum, eventually developing into the soft mode. Another model was presented by Raich and Bernstein [9] in which the authors considered the torsional degree of freedom only, and, starting from the single particle susceptibility of a one-dimensional rotor, they looked for the lattice instability. Heine

† Permanent address: Institute of Nuclear Physics, Radzikowskiego 152, 31-342 Kraków, Poland.

0953-8984/92/296241+12$04.50

and Price [10] developed a model of mutually intermeshed phenyl ring rotations that lead to an incommensurate structure caused by orientation frustration. The model was then extended to elevated pressures in order to obtain a phase diagram [11].

A priori the same instability should appear in all polyphenyls. Indeed, all these compounds have similar crystalline structures in the high-temperature phase ($P2_1/a$) [1]. In fact the paper by Raich and Bernstein [9] tries to explain the phase transitions in biphenyl and p-terphenyl in a consistent way. However, there are substantial differences between these two phase transitions. The phase transition in biphenyl is displacive, with a well-defined soft mode [1, 2], whereas the phase transition in terphenyl is of the order–disorder type with a critical relaxation mode [1]. Applying hydrostatic pressure enhances displacive character of the phase transition. In biphenyl the transition remains continuous and the displacive limit ($T_c = 0$) is reached at pressures just below 2 kbar [12]. With increasing pressure the phase transition in p-terphenyl changes from order–disorder to displacive type [12, 13]. However, the transition becomes more and more discontinuous and a third phase has been discovered below the triple point [1]. Finally, the low-temperature phases of biphenyl are incommensurate with wave vectors inside the Brillouin zone while in p-terphenyl they become superstructure with wave vectors at the zone boundary. In this paper we present lattice dynamics calculations of biphenyl and p-terphenyl that are a continuation of the model formulated earlier by Plakida *et al* [14].

2. Model

We performed lattice dynamics calculations in the rigid phenyl ring approximation, for which the potential needed was:

$$V = V_{\text{intra}} + V_{\text{inter}} \tag{1}$$

where V_{inter} represents intermolecular interactions while V_{intra} represents interactions between phenyl rings of the same molecule. The latter is harmonic except in the case of torsional degrees of freedom where we apply the double-well potential:

$$V_{\text{intra}}(\varphi) = \tfrac{1}{2}A\varphi^2 + \tfrac{1}{2}B\varphi^4 \tag{2}$$

where $A < 0$ and $B > 0$ and are the parameters to be adjusted. A similar potential was used in the paper of Benkert *et al* [15]. In the next step we make the approximation [16]:

$$\varphi^4 \approx \varphi^2\langle\varphi^2\rangle \tag{3}$$

where

$$\langle\varphi^2\rangle = \int \mathrm{d}\omega\, g_t(\omega)\frac{\coth(\omega/2T)}{2\omega} \tag{4}$$

is the mean square amplitude of the torsional motion at the temperature T and $g_t(\omega)$ is the density of states projected onto the torsional degree of freedom. Hence, the effective intramolecular potential for the torsional motion is clearly seen to be temperature dependent. It is also coupled to the whole phonon system via $g_t(\omega)$.

The other degrees of freedom are temperature independent. Since it is just the local part of the potential that depends on the temperature, unlike in other self-consistent phonon models, there is no thermal expansion of the lattice. All the calculations were performed for deuterated samples for comparison with the very rich results of neutron scattering. As is explained below, some of the calculations were also done for non-deuterated (hydrogenated) substances (e.g. quantum effects under pressure). In our approximation the potential is the same in either case. The main difference between our model and those of Heine and Price [10] and Raich and Berstein [9] is that we take into account all modes that may play a role in the phase transition. As will be shown in section 5 this is necessary for understanding the incommensurate structure. The quantum statistics in (4) is essential for the understanding of the phase diagram at the low-temperature limit.

3. Potential parameters and calculation procedure

The intermolecular part of the potential was expressed as a sum of the atom–atom interactions of the form '$6-\exp$' using the parameters given by Williams [17]. The parameters are the same as those used in the paper by Takeuchi *et al* [7] and only slightly different from the ones used by Heine and Price [10]. For torsion measurements the parameters A and B were adjusted at two points on the p–T phase diagram of solid biphenyl: $p = 0$, $T = 38$ K and $p = 1$ kbar, $T = 20$ K. The values of the parameters are:

$$A = -33.956 \qquad B = 1610.3 \qquad \langle\varphi^2\rangle = 0.003 \qquad \text{at } T = 38 \text{ K} \tag{5}$$

in energy units of kcal mol^{-1} and angle units of radians. It must be stressed that our intramolecular potential is an effective one. Due to the fact that our parameters were adjusted with the intermolecular part of the potential in a self-consistent way, one should not compare them directly with other models (e.g. see table 3 from [15]). Our parameters correspond to the effective twist potential with two minima at $\pm 5.9°$, with the barrier between the two being 0.09 kcal mol^{-1}. All the calculations were performed at the interaction energy minimum with respect to the structural parameters. This minimum depends on pressure, hence the unit cell parameters and the molecular orientations depend on pressure as well. When performing the pressure sensitive calculations we are interested in the Gibbs free energy rather than the Helmholtz free energy. We have to minimize the expression:

$$G = \langle V\rangle + pv \tag{6}$$

where v is the unit cell volume, p is the pressure and $\langle V\rangle$ the effective potential. The potential parameters themselves do not depend on pressure. As mentioned earlier, there is no temperature dependence of the unit cell or of the molecular orientation. Lattice dynamics calculations were performed for the 128 points in the Brillouin zone defined by Chadi and Cohen [18]. This method was found to be the most effective by Bonadeo and Burgos [19]. All points have the same weight and take the values: $\frac{1}{8}, \frac{3}{8}, \frac{5}{8}, \frac{7}{8}$. The phase transition was interpreted as a point in the p–T plane where $\omega(q)$ is equal to zero for some wave vector, q.

4. Results

4.1. Phonon dispersion curves

As mentioned in the previous section, the unit cell parameters depend on pressure but not on temperature. The calculated pressure dependence of the unit cell parameters a, b and c is shown in figure 1. For all three directions the calculated compressibility coefficients are roughly the same, varying from 0.002 to 0.004 kbar^{-1}, and remain in very good agreement with the results of the neutron experiment [20, 21]. The changes with pressure of the monoclinic angle β are very slight. The phonon dispersion curves for biphenyl at $p = 0$ are shown in figure 2. They are plotted for the wave vector q along the symmetry axis b^* and for the Brillouin zone boundary. For clarity, $q \parallel b^*$ phonon modes are divided according to their being symmetric or antisymmetric with respect to the twofold axis. It is clearly seen that the phonon branch that is symmetric with respect to the twofold axis has a deep minimum at about $q = 0.4b^*$. This result is in agreement with the experimentally determined structure of phase III [22]. So the structure of phase III is $P_{\bar{1}}^{Pa}$ rather than $P_{1\bar{1}}^{P2_1/a}$. However, the lowest point on the $\omega(q)$ surface is at the general point in the Brillouin zone: $q_c = (-0.02, 0.40, 0.22)$. This value should be compared with the experimentally found modulation vector of the biphenyl phase II, which is incommensurate; the experimental value is: $(-0.07, 0.45, 0.13)$ [23]. As was explained in section 2, all the interphenyl modes were calculated. For clarity, only the lowest eight branches are plotted; these include external modes of biphenyl molecules and the two torsional modes. Those modes inside the Brillouin zone are mixed-type modes. Close inspection of the eigenvectors of the dynamical matrix allows us to see the character of a given mode. A mode that goes soft at $q = q_c$ is predominantly torsional in character, admixed with translation of the molecule along its long axis and slight reorientation of the whole molecule. The eigenvector of the soft mode is explicitly given in the appendix. The detailed shape of the minimum of the dispersion surface is shown in figure 3. It is clearly seen that the dispersion along the direction b^* is much stronger than that along a^* and c^*. The slope of the soft phonon branch at $T = T_c$ should roughly correspond to phason excitation in phase II. The dispersion law in the vicinity of q_c can be perfectly parameterized in the following way [24]:

$$\omega^2(q, T) = \omega_0^2(T - T_c) + \alpha_H q_1^2 + \alpha_K^2 q_2^2 + \alpha_L^2 q_3^2. \tag{7}$$

The calculated values: $\alpha_H = 6, \alpha_K = 27$ and $\alpha_L = 7$ should be compared with the experimental ones: $\alpha_H = 4, \alpha_K = 22$ and $\alpha_L = 1$ in units of THz^{2}Å^2 [24].

4.2. Pressure dependence

As explained earlier, pressure enters the calculations via minimization of the structure. The pressure dependence of the phonon modes is weak and can be explained by the Grüneisen parameter. The soft mode is the only one for which the pressure dependence is dramatic. Its behaviour at $T = 3$ K is shown in figure 4. Again, very good agreement with the experiment is observed, and the value 0.1 THz^2 kbar^{-1} is obtained [20].

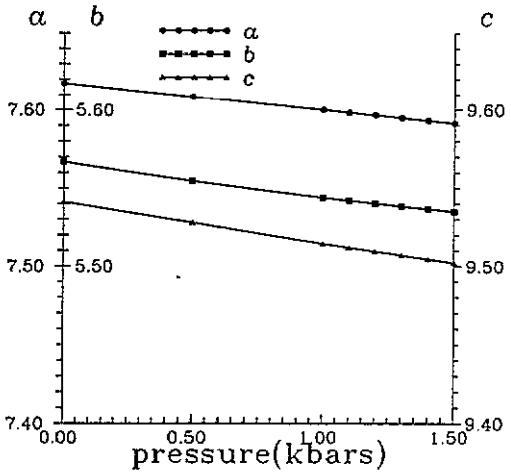

Figure 1. Calculated pressure dependence of the monoclinic unit cell parameters a, b and c in units of Å.

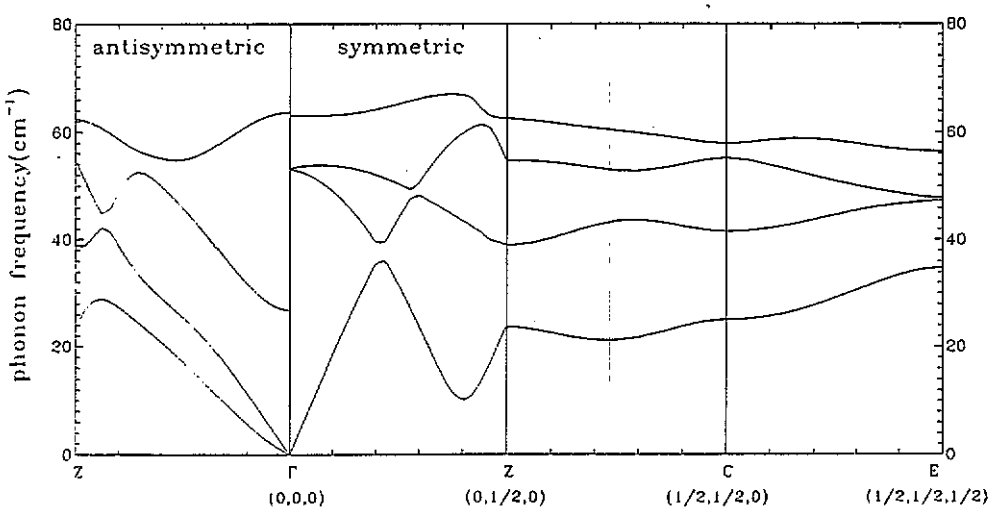

Figure 2. Phonon dispersion curves for biphenyl at $p = 0$ and $T = 38$ K.

4.3. Temperature dependence

The only mode in our model that depends on temperature is the torsional one. Figure 5 shows how the soft mode at $p = 0$ depends on temperature. The temperature dependence of ω^2 is observed to be almost linear.

4.4. Phase diagram

The phonon calculation for different temperatures and pressures allows us to establish a phase diagram on the p–T plane. The phase transition is located at the zero-phonon frequency at finite wave vector q_c. As already mentioned in section 3, the parameters A and B of the local torsional potential were fitted so that the phase transitions occur at $p = 0$, $T = 38$ K and $p = 1$ kbar, $T = 20$ K. The full diagram is presented in figure 6; its character agrees very well with the experimental one [24]. For temperatures greater than 20 K, T_c decreases linearly with increasing

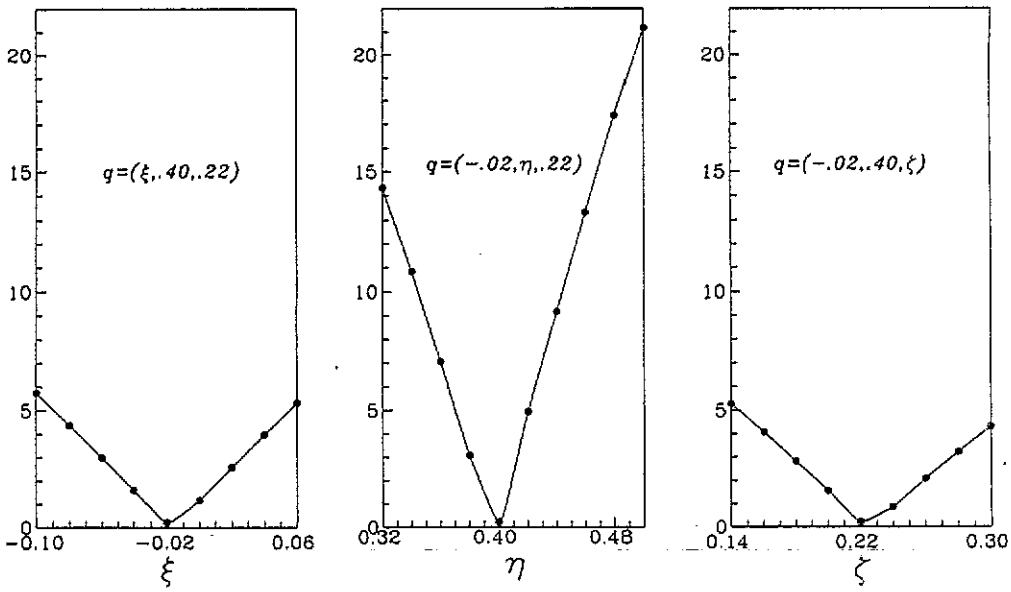

Figure 3. Phonon dispersion in the vicinity of q_c along three main directions a^*, b^* and c^*. Phonon frequencies are in units of cm^{-1}.

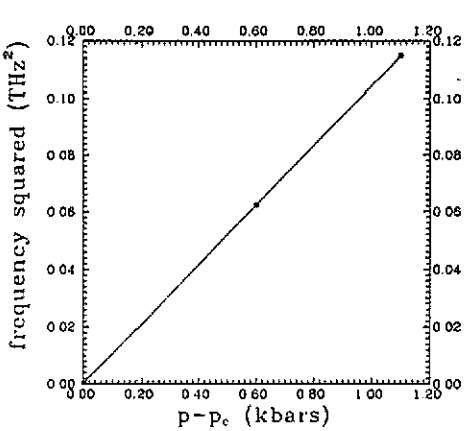

Figure 4. Pressure dependence of the squared frequency of the soft mode at $T = 3$ K. Experimental points are taken from [21].

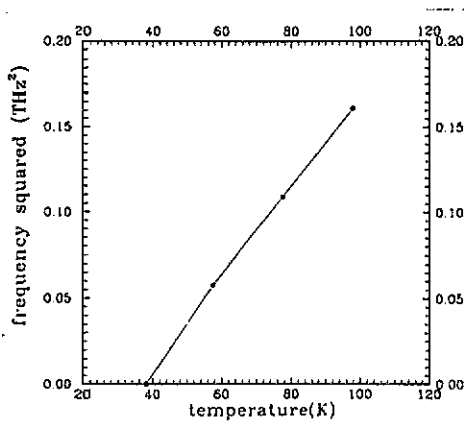

Figure 5. Temperature dependence of the squared frequency of the soft mode at $p = 0$. Experimental points are taken from [21].

pressure; below 20 K it decreases more rapidly and finally reaches the quantum limit $p = 1.5$ kbar at $T = 1$ K. This low temperature behaviour is a direct consequence of the zero-point motion of (4). Assuming the same potential parameters for non-deuterated biphenyl we calculated the phase diagram for $C_{12}H_{10}$; the result is also shown in figure 6. In this case, the phase transition occurs systematically at lower temperatures than for the deuterated substance. This might be a direct manifestation of the fact that some other effects (e.g. the C–H bond lengths being slightly bigger than C–D distances) were neglected . The phase diagram for the hydrogenated

compound was not measured in detail, but at $p = 0$, $T_c = 40$ K the phase transition occurs 2 K higher than for the deuterated substance. Because of quantum effects dominant at low temperatures one can expect crossing of the phase boundary lines for some temperatures. Then, for $T_c \approx 0$ K, p_c for the hydrogenated substance should be lower than for the deuterated one. In the classical approximation which is valid for $T_c \gg \omega_D$ the critical temperature T_c does not depend on the isotope substitution. The detailed discussion of the pressure influence on the phase transition given in [25] is fully confirmed by our calculations. We hope to deal with the problem of the phase transition between phases II and III in another paper.

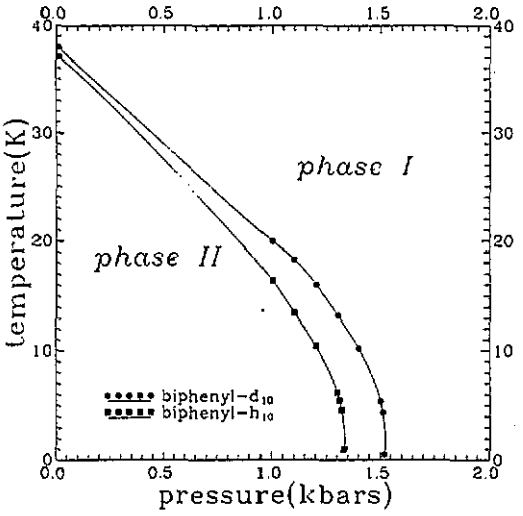

Figure 6. Calculated phase diagram of biphenyl. Experimental points are taken from [20].

5. The structure of phase II

Knowledge of the critical wave vector q_c and the eigenvector of the soft mode allows us to explain the low temperature structure of biphenyl. Since the wave vector is at a general point in the Brillouin zone of the monoclinic space group, the full star consists of four arms, and the active representation is four dimensional. The arms are

$$q_1 = (q_x, q_y, q_z) \qquad q_2 = (-q_x, q_y, -q_z) \qquad q_3 = -q_1 \qquad q_4 = -q_2. \tag{8}$$

The free-energy density has the form discussed by Cowley [26]:

$$F = F_0 + \tfrac{1}{2}a(T - T_c)(Q(q_1)Q(q_3) + Q(q_2)Q(q_4)) + b(Q^2(q_1)Q^2(q_3) + Q^2(q_2)Q^2(q_4)) + cQ(q_1)Q(q_2)Q(q_3)Q(q_4) \tag{9}$$

where

$$Q(q_3) = Q^*(q_1) \qquad \text{and } Q(q_4) = Q^*(q_2). \tag{10}$$

By substituting:

$$Q(q_1) = A_1 e^{i\varphi} \tag{11}$$

$$Q(q_2) = A_2 e^{i\phi} \tag{12}$$

into (9) we obtain the simplified form of the free-energy density:

$$F = F_0 + \tfrac{1}{2}a(T - T_c)(A_1^2 + A_2^2) + b(A_1^4 + A_2^4) + cA_1^2A_2^2. \tag{13}$$

The minimum of the free energy is realized by the following solutions:

for $b > 0, c > 2b$ $\quad A_1 \neq 0, A_2 = 0$ or $A_1 = 0, A_2 \neq 0$ (14)

for $b > 0, -2b < c < 2b$ $\quad A_1 = A_2$ (15)

for all other b and c $\quad A_1 = A_2 = 0.$ (16)

Solution (16) corresponds to the high-temperature symmetric phase. Solution (14) corresponds to the bidomain structure which is stripe-like. Solution (15) corresponds to the monodomain structure with bidimensional modulation which is quilt-like. On the basis of their own model and a Landau-type expansion, Benkert and Heine [27] argued that the stripe-like structure is favourable. The phenomenological treatment of Parliński *et al* [28] also suggested a stripe-like structure. Finally, the experimental work of Launois *et al* [24] supports the stripe-like structure in phase II of biphenyl. We investigated which of these has lower energy by calculating the potential energy of a given structure using the distortion given by the eigenvector of the soft mode. In our calculations both intramolecular and intermolecular potentials contribute to the fourth-order term in free energy, so the relation between the constants b and c is rather complicated. Since the translational symmetry in the incommensurate phase is lost, additional integration over the phase shift was performed:

$$V = \int_{-\pi}^{\pi} d\tau \sum_{k,k'} v(k, k', \tau) \tag{17}$$

where k and k' label molecules and τ is the phase shift. More details about computational aspects are given in the appendix. The results of the calculations are shown in figure 7. The upper curve represents the quilt-like structure while all other curves represent stripe-like structures at different temperatures. Evidently the calculations show that the structure with unidimensional modulation has lower energy. It should be pointed out that neglecting degrees of freedom other than torsion leads to a quilt-like structure. The most striking feature is that at $T = T_c$ the energy plot has a double minimum character. This means that the expectation value $\langle Q \rangle \neq 0$ at $T = T_c$. Exactly why we obtained a discontinuous phase transition starting from the Landau Hamiltonian is not obvious. Bruce [29] discussed the problem and finally concluded that this was an artifact of the self-consistent phonon approximation. The maximal twist angle between phenyl rings estimated from the calculation at 20 K is $\cong 10°$.

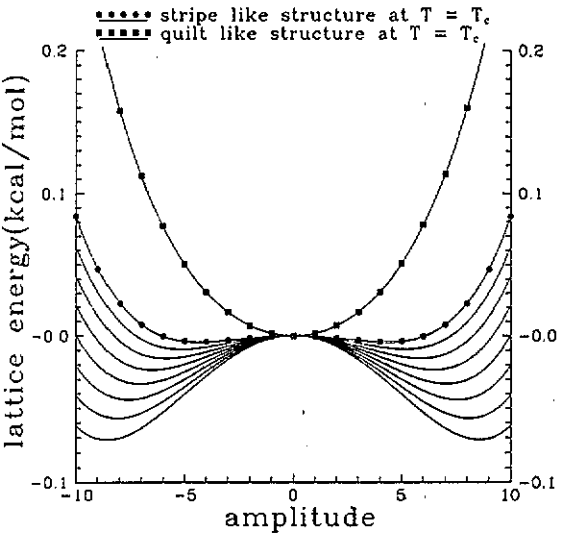

Figure 7. Lattice energy of the two possible structures of the incommensurate phase II. The upper curve corresponds to a quilt-like structure; the lower curves correspond to stripe-like structures at different temperatures.

6. P-terphenyl

The same model was applied for p-terphenyl under pressure. The model is supposed to work well for a displacive-type phase transition, of which p-terphenyl under pressure is one case [20]. However the model predicts a continuous phase transition, while it is known from experiment [13] that the phase transition in p-terphenyl becomes first order when pressure is applied. Nevertheless phonon dispersion curves show quite good agreement with experiment. In particular, there is one phonon branch in the Brillouin zone with almost no dispersion between points $(\frac{1}{2}, \frac{1}{2}, 0)$ and $(\frac{1}{2}, \frac{1}{2}, \frac{1}{2})$ that has very low energy. In fact there is a triple point on the phase diagram at $T = 70$ K and $p = 3.5$ kbar joining the phase boundary between phases I, II and III. The phase transition between phases I and III takes place at $q = (\frac{1}{2}, \frac{1}{2}, \frac{1}{2})$; the phase transition between phases I and II takes place at $q = (\frac{1}{2}, \frac{1}{2}, 0)$. The point symmetries of phases II and III are the same; they differ by translational symmetry only. The phonon dispersion curves for p-terphenyl at $p = 4$ kbar are shown in figure 8. One can easily see all the similarities and differences between this and biphenyl. It should be noted that only external modes and two twist modes are plotted for clarity. The very small dispersion on the Brillouin zone surface perpendicular to b^* (see figure 8) indicates weak coupling between molecules in the ac plane. With all the limitations mentioned above we can calculate the temperature of phonon instability. Taking the same potential parameters A and B as for biphenyl we obtain the $T_c \approx 111$ K at $p = 0$, which is much lower than the experimental $T_c = 180$ K.

7. Conclusions

The model presented here accurately describes the phase transition between the high temperature phase I and phase II, which is incommensurate in biphenyl. It estimates

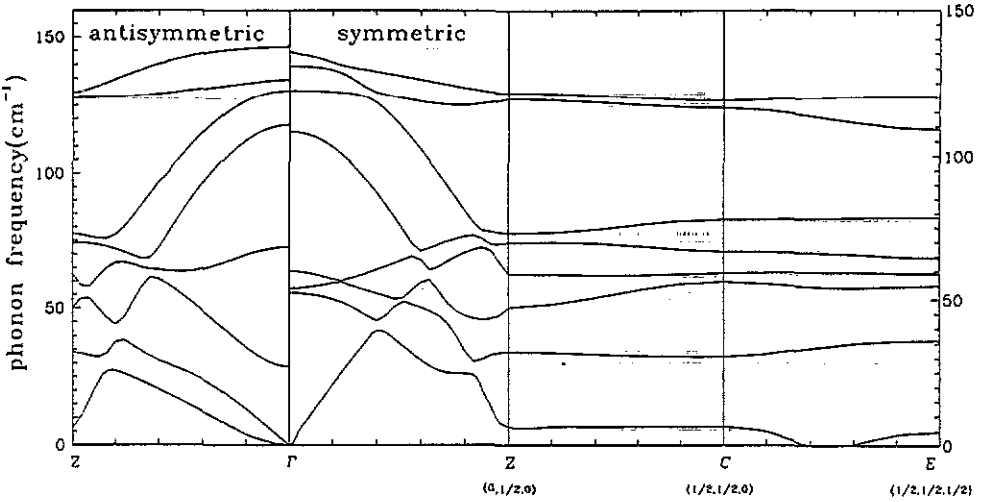

Figure 8. Phonon dispersion curves for p-terphenyl at $p = 4$ kbar.

the critical wave vector, pressure and temperature dependence of the soft mode quite well and allows us to reproduce the phase diagram. The phonon dispersion of the soft mode is very well reproduced. The model also provides information about the structure of phase II. Although the para p-terphenyl case is more complicated, the model does give a qualitative explanation of the phase transitions in this substance.

Acknowledgments

One of the authors (TW) is grateful for the hospitality of the staff of Laboratoire de Physique Cristalline, Université de Rennes and to CNRS for financial support.

Appendix

The results of the lattice energy calculations presented in figure 8 were obtained as follows: the soft phonon is characterized by the wave vector

$$q_1 = (-0.02, 0.40, 0.22) \tag{A1}$$

and by the (complex) eigenvector:

$$U_1^{\text{trans}}(1) = \begin{pmatrix} -0.003 \\ 0.008 \\ 0.000 \end{pmatrix} \qquad U_1^{\text{rot}}(1) = i * \begin{pmatrix} 0.007 \\ -0.004 \\ -0.004 \end{pmatrix} \qquad U_1^{\text{tors}}(1) = 0.046 \tag{A2}$$

$$U_1^{\text{trans}}(2) = \begin{pmatrix} -0.004 \\ 0.010 \\ -0.035 \end{pmatrix} \qquad U_1^{\text{rot}}(2) = i * \begin{pmatrix} -0.009 \\ -0.006 \\ 0.002 \end{pmatrix} \qquad U_1^{\text{tors}}(2) = -0.056 \tag{A3}$$

and by $U_2^j(m)$ where $j = (\text{trans, rot, tors})$ and $m = 1, 2$ for the wave vector q_2. The wave vectors q_1 and q_2 are symmetry related as are U_1 and U_2. The $U^{\text{trans}}(m)$ and $U^{\text{rot}}(m)$ are expressed in the orthogonal crystal frame a, b, c^* and are normalized to mass and moment of inertia respectively:

$$(U^j(m))^+ M_j(m) U^j(m) = 1 \tag{A4}$$

where M_{trans} is the mass, M_{rot} is the moment of inertia of the whole molecule, m, and M_{tors} is the moment of inertia of the torsional mode.

We then displace the molecule m in the unit cell l :

$$u^j(m,l) = \text{amplitude} * \left(U_1^j(m) \exp(\mathrm{i} q_1 (l + x_m + \varphi_1)) \right) \tag{A5}$$

in the case of unidimensional modulation, or

$$\begin{aligned} u^j(m,l) = \text{amplitude} * (&U_1^j(m) \exp(\mathrm{i} q_1 (l + x_m) + \varphi_1) \\ &+ U_2^j(m) \exp(\mathrm{i} q_2 (l + x_m) + \varphi_2)) \end{aligned} \tag{A6}$$

in the case of bidimensional modulation. The free phases φ_1 and φ_2 reflect the fact that the modulation is incommensurate. In the next step we calculate the lattice energy as a sum of the atom–atom interaction and the intermolecular energy

$$V = \int_{-\pi}^{\pi} \mathrm{d}\varphi_1 \sum_{m,m'} V(m, m', \varphi_1) \tag{A7}$$

or

$$V = \int_{-\pi}^{\pi} \mathrm{d}\varphi_1 \, \mathrm{d}\varphi_2 \sum_{m,m'} V(m, m', \varphi_1, \varphi_2) \tag{A8}$$

for unidimensional and bidimensional modulation respectively. The integration was carried out by means of the ten-point Gaussian quadrature.

References

[1] Cailleau H, Baudour J L, Meinnel J, Dworkin A, Moussa F and Zeyen C M E 1980 *Faraday Discuss. Chem. Soc.* **69** 7

[2] Cailleau H 1986 *Incommensurate Phases in Dielectrics* vol 2, ed R Blinc and A P Levanyuk (Amsterdam: North-Holland) p 71 and references therein

[3] Venkatamaran G and Sahni V S 1970 *Rev. Mod. Phys.* **42** 409

[4] Pawley G S and Cyvin S J 1970 *J. Chem. Phys.* **52** 4073

[5] Califano S, Schettino V and Neto N 1981 *Lattice Dynamics of Molecular Crystals* (Berlin: Springer)

[6] Burgos E, Bonadeo H, and D'Alessio E 1976 *J. Chem. Phys.* **65** 2460

[7] Takeuchi H, Suzuki S, Dianoux A J and Allen G 1981 *Chem. Phys.* **55** 153

[8] Wasiutyński T, Natkaniec I and Belushkin A V 1981 *J. Physique Coll.* C6 589

[9] Raich J and Bernstein E R 1984 *Mol. Phys.* **53** 597

[10] Heine V and Price S 1985 *J. Phys. C: Solid State Phys.* **18** 5259

[11] Benkert C 1987 *J. Phys. C: Solid State Phys.* **20** 3369

[12] Launois P, Girard A, Cailleau H, Moussa F, Toudic B, Delugeard Y, Baudour J L, Bernard L, Vettier C, Serve R and Mons J 1987 *Dynamics of Molecular Crystals* ed J Lascombe (Amsterdam: Elsevier) p 155

[13] Girard A, Delugeard Y and Cailleau H 1987 *J. Physique* **48** 1751
[14] Plakida N M, Belushkin A V, Natkaniec I and Wasiutyński T 1983 *Phys. Status Solidi* b **118** 129
[15] Benkert C, Heine V and Simmons E H 1987 *J. Phys. C: Solid State Phys.* **20** 3337
[16] Plakida N M 1973 Metod funkcji greena *Statistical Physics and Quantum Field Theory* ed N N Bogollyubov p 111 (in Russian)
[17] Williams D E 1966 *J. Chem. Phys.* **45** 3770
[18] Chadi D J and Cohen M L 1973 *Phys. Rev.* B **8** 5747
[19] Bonadeo H and Burgos E 1982 *Acta Crystallogr.* A **38** 29
[20] Lemée-Cailleau M H 1989 Etude, sous pression, de transitions de phase dans des cristaux moleculaires *PhD thesis* Université de Rennes I
[21] Launois P 1987 Etude par diffusion inelastique de neutrons et sous pression hydrostatique de la dynamique des phases cristallines des parapolyphenyles *PhD Thesis* Université de Paris Sud Centre d'Orsay
[22] Baudour J L and Sanquer M 1983 *Acta Crystallogr.* B **39** 75
[23] Cailleau H, Messager J C, Moussa F, Bugaut F, Zeyen C M E and Vettier C 1986 *Ferroelectrics* **67** 3
[24] Launois P, Moussa F, Lamée-Cailleau M H and Cailleau H 1989 *Phys. Rev.* B **40** 5042
[25] Braeter H, Plakida N M and Windsch W 1988 *Solid State Commun.* **67** 1219
[26] Cowley R A 1980 *Adv. Phys.* **29** 1
[27] Benkert C and Heine V 1987 *J. Phys. C: Solid State Phys.* **20** 3355
[28] Parliński K, Schranz W and Kabelka H 1989 *Phys. Rev.* B **39** 488
[29] Bruce A D 1980 *Adv. Phys.* **29** 111